Monthly Notices
of the
ROYAL ASTRONOMICAL SOCIETY

MNRAS **480,** 2704–2718 (2018)
Advance Access publication 2018 July 27

doi:10.1093/mnras/sty2035

Predicting the binary black hole population of the Milky Way with cosmological simulations

A. Lamberts,[1]★ S. Garrison-Kimmel,[1] P. F. Hopkins,[1] E. Quataert,[2] J. S. Bullock,[3] C.-A. Faucher-Giguère,[4] A. Wetzel,[5] D. Kereš,[6] K. Drango[1] and R. E. Sanderson[1]

[1]*Theoretical Astrophysics, California Institute of Technology, Pasadena, CA 91125, USA*
[2]*Department of Astronomy and Theoretical Astrophysics Center, University of California, Berkeley, CA 94720, USA*
[3]*Center for Cosmology, Department of Physics and Astronomy, University of California, Irvine, CA 92697, USA*
[4]*Department of Physics and Astronomy and CIERA, Northwestern University, Evanston, IL 60208, USA*
[5]*Department of Physics, University of California, Davis, CA 95616, USA*
[6]*Department of Physics, Center for Astrophysics and Space Science, University of California at San Diego, 9500 Gilman Drive, La Jolla, CA 92093, USA*

Accepted 2018 July 25. Received 2018 July 20; in original form 2018 January 8

ABSTRACT

Binary black holes are the primary endpoint of massive stars. Their properties provide a unique opportunity to constrain binary evolution, which remains poorly understood. We predict the main properties of binary black holes and their merger products in/around the Milky Way. We present the first combination of a high-resolution cosmological simulation of a Milky Way-mass galaxy with a binary population synthesis model in this context. The hydrodynamic simulation, taken from the FIRE project, provides a cosmologically realistic star formation history for the galaxy, its stellar halo, and satellites. During post-processing, we apply a metallicity-dependent evolutionary model to the star particles to produce individual binary black holes. We find that 7×10^5 binary black holes have merged in the model Milky Way, and 1.2×10^6 binaries are still present, with a mean mass of $28\,M_\odot$. Because the black hole progenitors are strongly biased towards low-metallicity stars, half reside in the stellar halo and satellites and a third were formed outside the main galaxy. The numbers and mass distribution of the merged systems is broadly compatible with the LIGO/Virgo detections. Our simplified binary evolution models predict that *LISA* will detect more than 20 binary black holes, but that electromagnetic observations will be challenging. Our method will allow for constraints on the evolution of massive binaries based on comparisons between observations of compact objects and the predictions of varying binary evolution models. We provide online data of our star formation model and binary black hole distribution.

Key words: gravitational waves – binaries: close – stars: black holes – Galaxy: abundances – Galaxy: stellar content.

1 INTRODUCTION

The global properties of compact objects (COs) in the Milky Way (MW) provide crucial information on the star formation history of the Galaxy as well as on stellar evolution. Broadly speaking, stars born with mass $M < 8\,M_\odot$ evolve into white dwarfs (WDs), those of $M \simeq 8$–20 evolve into neutron stars (NSs), and those above $\simeq 20\,M_\odot$ turn into black holes (BHs; e.g. Fryer 1999, but also see Sukhbold et al. 2016), though stars between $\simeq 120$ and $250\,M_\odot$ may undergo a pair instability supernova that leaves no remnant (Fryer et al. 2012). Aside from systems that have undergone mergers or left the Galaxy due to BH kicks (Janka 2013), the number of compact remnants quantifies past star formation. The localization of COs within a galaxy may also be indicative of the progenitor's formation conditions (lookback time, local environment, and metallicity). The mass distributions, orbital properties, and/or proper motion of the COs can inform us on stellar evolution and explosion mechanisms. In this paper, we provide detailed predictions for the expected binary black hole (BBH) population and their merger products in the MW, as well as some observational properties.

The current ($z = 0$) population of BHs is particularly important as BHs evolve from the most massive stars, whose short lives mean that we can only directly observe the population that formed within the last $\sim 20\,$Myr. In particular, BHs provide unique information on the initial mass function of massive stars, which are key

★ E-mail: lamberts@caltech.edu

drivers of galactic evolution through chemical enrichment, stellar winds, ionizing radiation, and their final explosions (Muratov et al. 2015; Geen et al. 2015). Observations indicate that most, if not all massive stars form in binary systems (Sana et al. 2012), with recent work suggesting that binaries are even more ubiquitous for lower metallicity stars (Badenes et al. 2018). As such, the properties of stellar BHs can also inform us about crucial phases of binary evolution such as supernova kicks and mass transfer (see Postnov & Yungelson 2014 for a recent review on compact binary formation).

Unfortunately, the inventory of stellar mass BHs in the MW is far from complete. So far, the only confirmed systems are found in X-ray binaries, where the BHs manifest themselves through accretion of material from a companion star (see Casares, Jonker & Israelian 2017 for a recent review). About 60 of these systems have been detected around low-mass companion stars, and a handful around massive stars (Corral-Santana et al. 2016). The latter are systems formed within the last 20 million years and possible progenitors to BBHs. The astrometric mission *Gaia* could detect more than 10 000 BHs around stellar companions (Breivik, Chatterjee & Larson 2017; Mashian & Loeb 2017). Based on the observed BBH merger rate from Abbott et al. (2016c), Elbert, Bullock & Kaplinghat (2018) estimate that there could be up to 100 million BHs in the MW. So far, however, no BH has been observed in a binary with another compact object in the MW.

Similarly, there have been no firm detections of stellar mass BHs without a stellar companion in the MW. Such BHs are not expected to emit electromagnetic radiation unless they are accreting from a dense environment (Agol & Kamionkowski 2002; Maccarone 2005). Future hard X-ray surveys or radio observations with the *Square Kilometer Array (SKA)* could lead to the first such detections, if the accretion rates and radiative efficiencies are high enough (Fender, Maccarone & Heywood 2013; Corbel et al. 2015). Ioka et al. (2017) further suggest that BHs formed out of merged BBHs should have a high spin and may thus produce gamma-ray emission in a jet. Year-long microlensing events with no visible lens have been tentatively attributed to BHs in the galactic bulge (Wyrzykowski et al. 2011, 2016).

Gravitational waves may be the most promising means of detecting BBHs in the MW. The first direct detection of GWs came from the merger of two stellar mass BHs (GW150914) via the Laser Interferometry Gravitational wave Observatory (LIGO; Abbott et al. 2016b), with a handful of similar detections following. Several studies propose to distinguish binary evolution channels using observational properties of compact object mergers from gravitational waves (Belczynski, Kalogera & Bulik 2002; Voss & Tauris 2003; Belczynski et al. 2008; Dominik et al. 2012; Stevenson, Ohme & Fairhurst 2015; Mapelli et al. 2017). With LIGO/Virgo, we observe the very last moments (of order of a few seconds or less) before the BBH merges, the merger itself, and the ringdown of the newly formed (and more massive) BH. Given the very short signal in comparison to the very long inspiral time of a BBH, the likelihood of detecting one of these events in the MW is close to zero.

The high masses of GW150914, $M_1 = 36^{+5}_{-4}\,\mathrm{M}_\odot$, $M_2 = 29 \pm 4\,\mathrm{M}_\odot$, suggest a low-metallicity progenitor binary (Belczynski et al. 2008; Dominik et al. 2013), with $Z \lesssim 0.1\,\mathrm{Z}_\odot$ (Belczynski et al. 2016) colorblack although $Z \lesssim 0.5\,\mathrm{Z}_\odot$ may be possible for very massive progenitors (Abbott et al. 2016d; Eldridge & Stanway 2016). Based on an analytic model, we showed in Lamberts et al. (2016) that the progenitors of GW150915 most likely formed either relatively recently in a dwarf galaxy (stellar mass $\lesssim 10^7\,\mathrm{M}_\odot$), or around the peak of cosmic star formation ($\simeq$10 Gyr ago) in a galaxy that would now resemble the MW (stellar mass $\sim 10^{10}$–$10^{11}\,\mathrm{M}_\odot$). Mapelli et al. (2017) and Schneider et al. (2017) found similar results when combining a binary evolution model with the Illustris simulation and with a high-resolution dark matter-only simulation, respectively. While lower mass BBHs can be formed out of higher metallicity progenitors, BBHs are strongly biased towards sub-solar metallicity environments, as the amount of mass-loss from stellar winds scales with metallicity (Belczynski et al. 2010a; Dominik et al. 2013). As such, we expect the BBH population of the MW to have a different spatial distribution than the overall stellar mass.

Current predictions for the binary compact object population of the MW are based on simplified models for its star formation history, metallicity, and morphology. The MW is often approximated by a spherically symmetric bulge and a disc with a characteristic scale height (e.g. Nelemans et al. 2001; Ruiter et al. 2010; Liu & Zhang 2014). The star formation rate in the disc is typically assumed to be constant over time and to occur at fixed metallicity (solar). The stellar halo is rarely included (except in Belczynski, Benacquista & Bulik 2010b, where the halo is assumed to form in a single burst 13 Gyr ago with a single metallicity). The inaccuracies resulting from these approximations are compounded by the uncertainties in the binary evolution models, such that it is extremely difficult to constrain binary evolution through comparisons between predictions from these simplified Galaxy models and observations.

These simplifications motivate the present analysis, where we instead apply a population synthesis model to the star formation history of a cosmological, hydrodynamic simulation of a MW-mass galaxy, first presented in Wetzel et al. (2016). Although the simulation does not specifically aim to reproduce the exact morphology of the MW, it includes a cosmologically realistic star formation and merger histories, satellite population, and stellar halo, and a self-consistent metal enrichment and gas exchange with the circumgalactic and extragalactic media. An exact prediction for the BBH distribution in the MW requires observational constraints on the ages and metallicities of the entire stellar population of the MW, and would be particularly sensitive to the oldest (and therefore faintest) stars. Unfortunately, this detailed information will remain out of reach for some time, especially outside the disc of the Galaxy. In the meantime, our technique should yield a BBH population that is statistically consistent with that of the MW.

The *Laser Interferometer Space Antenna (LISA)*, a space-based mission led by ESA and scheduled to launch in the mid-2030s, will provide the first view of the double compact object (DCO) population in the MW. With its 2.5 million km arms, the interferometer will be mostly sensitive to gravitational wave frequencies $10^{-4} \lesssim f_{\mathrm{GW}} \lesssim 10^{-1}$ Hz. One of *LISA's* main science goals is a first inventory of very short orbit DCOs in the MW. WD binaries with orbits shorter than an hour are expected to vastly dominate the signal (Nelemans et al. 2001; Ruiter et al. 2010), as they stem from more common low-mass stars and their formation likely has limited metallicity dependence. However, analytic estimates (Seto 2016; Christian & Loeb 2017) and binary population synthesis models combined with a multicomponent model for the Galaxy (Belczynski et al. 2010b; Liu & Zhang 2014) predict that at most a few BBH may be detected. However, Belczynski et al. (2010b) predict roughly 8.0×10^5 BBH in the Galaxy in their model A, where binaries survive the common envelope occurring during the Hertzprung gap. They predict roughly 5.6×10^5 binaries in model B, where common envelope mass transfer during the Hertzprung gap results

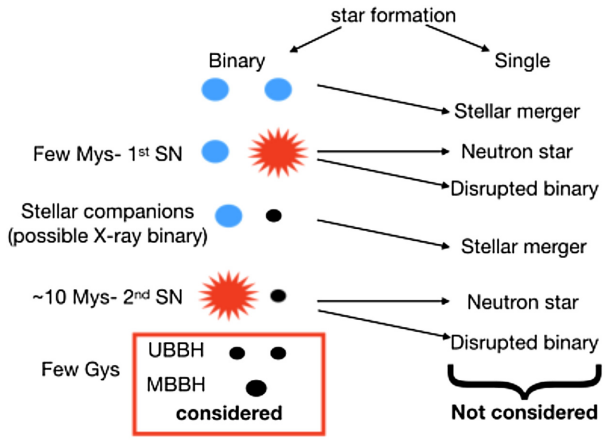

Figure 1. Possible endpoints of binary massive star formation. In this paper, we only focus on UBBH and MBBH, in red in the bottom left. We discard BHs from single stellar evolution, stellar mergers or binaries unbound by supernova kicks. We also do not consider BHs with WD, NS, or stellar companions. The above picture is a cartoon view to clarify the systems considered here and is not intended to be a precise representation of binary evolution.

in a stellar merger. In both cases, they predict most of the BBHs will be in the disc, a quarter of the systems in the bulge, and a negligible contribution from the halo. We will show that this arises directly from their neglect of more complex chemical and star formation history in the Galaxy. By applying a binary population synthesis model (similar to model B of Belczynski et al. 2010b) to a more realistic stellar population (both in terms of spatial distribution and age–metallicity space), we predict that a few tens of BBH will be detected in the MW with *LISA*.

In this paper, we provide a detailed view of the BH population resulting from BBHs systems in a MW-mass galaxy. We only focus on systems that survived BBH formation and are either unmerged binary black holes (UBBH) or merged binary black holes (MBBH). We do not consider BHs from single star formation, BHs resulting from binary systems disrupted by supernova kicks, BHs with a stellar companion, or single BHs formed after a stellar merger. We specifically consider UBBH+MBBH BHs and do not present earlier phases of binary evolution where BHs may have stellar companions emitting electromagnetic radiation. Fig. 1 summarizes the systems considered in this work.

We combine a high-resolution cosmological simulation of a MW-mass halo (Wetzel et al. 2016) with a binary population synthesis model (Section 2). We show how the progenitors of the BHs compare with the global population of stars and determine the properties of the BH population (Section 3). We present observational properties of both merged (i.e. currently single BHs) and unmerged systems (binary BHs), both with gravitational waves and electromagnetic methods (Section 4). We discuss the importance of a detailed model of the MW (Section 5) and conclude (Section 6).

2 METHODS

This paper emphasizes the importance of a realistic model for the star formation history for MW-mass galaxies with respect to previous studies of binary COs in the MW. We first present the key numerical and physical parameters of the simulation and show the physical quantities that are the most relevant to this study (Section 2.1). We then present the binary evolution model we use (Section 2.2) as well as our computation of GW emission (Section 2.3). We then explain how all these aspects are combined together (Section 2.4).

2.1 A realistic model of a MW-mass galaxy

The inputs to our binary evolution model (the ages, metallicities, and positions of star particles) are primarily drawn from the **m12i** FIRE-2 simulation, also known as 'Latte' (Wetzel et al. 2016). The simulation has an initial gas particle mass of 7070 $M_\odot$. The Latte simulation is part of the Feedback in Realistic Environment (FIRE; Hopkins et al. 2014) project,[1] specifically run using the improved 'FIRE-2' version of the code from Hopkins et al. (2018, for details, see Section 2 therein). The simulations use the code GIZMO (Hopkins 2015),[2] with hydrodynamics solved using the mesh-free Lagrangian Godunov 'MFM' method. For the gas, both the hydrodynamic and gravitational (force softening) resolutions are fully adaptive down to 1 pc. The simulations include cooling and heating from a meta-galactic background and local stellar sources from $T \sim 10$ to 10^{10} K. Star formation occurs in locally self-gravitating, dense, self-shielding molecular, Jeans-unstable gas. Stellar feedback from OB and AGB star mass-loss, type Ia and II supernovae, and multiwavelength photoheating and radiation pressure is directly based on stellar evolution models. Chemical enrichment stems from type Ia supernova (Iwamoto et al. 1999), core-collapse supernova (Nomoto et al. 2006), and O and AGB star winds (van den Hoek & Groenewegen 1997; Marigo 2001; Izzard et al. 2004). All the binary evolution models are included during post-processing, and the hydrodynamic simulation does not explicitly include binary effects.

The FIRE simulations reproduce the observed mean mass–metallicity relation both for stars and star-forming gas, between $z = 0$ and $z = 3$ (Ma et al. 2016) down to a stellar mass of 10^6 $M_\odot$. The simulations here include the subgrid-scale numerical turbulent metal diffusion terms described in Hopkins et al. (2018), which have almost no dynamical effect at the galaxy mass scales considered here (Su et al. 2017), but produce better agreement with the internal metallicity distribution functions observed in MW satellite galaxies (Escala et al. 2018).

Our main analysis is based on galaxy **m12i** (from Wetzel et al. 2016, though we analyse a re-simulation with turbulent metal diffusion first presented in Bonaca et al. 2017), chosen to have a relatively 'normal' merger history, but we also consider a lower-resolution version of **m12i** as well as two different galaxies **m12b** and **m12c** (Hopkins et al. 2018) at the same mass scale. **m12i** shows metallicity gradients (Ma et al. 2017) and abundances of α elements (Wetzel et al., in preparation) in the disc that are broadly consistent with observations of the MW. Its global star formation history is consistent with the MW (see Ma et al. (2017) for illustrations), although its present-day star formation rate of 6 $M_\odot$ yr^{-1} is somewhat higher than observed in the MW. The satellite distribution around the main galaxy in **m12i** presents a similar mass and velocity distribution as observed around the MW and M31, down to a stellar mass of 10^5 $M_\odot$, though the simulation does not contain an equivalent of the Large Magellanic Cloud; the most massive satellite is comparable to the Small Magellanic Cloud. Outputs from the simulation and corresponding mock *Gaia* catalogues are available online[3] (Sanderson et al. 2018).

[1] http://fire.northwestern.edu
[2] http://www.tapir.caltech.edu/~phopkins/Site/GIZMO.html
[3] https://fire.northwestern.edu/data/ and http://ananke.hub.yt

The simulation produces a catalogue of colorblack roughly 14 million particles of about $\simeq$7000 $M_\odot$ in mass.[4] For each particle, the quantities of interest here are its formation time t_*, metallicity Z, and position at $z = 0$ and at t_*. To determine the accretion rates of each BH associated with a star particle, we also recover the properties of the closest surrounding gas particle and assign it to the star particle. We consider only particles within 300 kpc of the centre of the main galaxy. This is slightly larger than the virial radius of the galaxy and allows us to largely sample the halo, satellites, and streams, while remaining unaffected by the boundaries of the high-resolution region.

The simulations assume a ΛCDM cosmology with $\Omega_\Lambda = 0.728$, $\Omega_\mathrm{m} = 0.272$, $\Omega_\mathrm{b} = 0.0455$, $h = 0.702$, $\sigma_8 = 0.807$, and $n_\mathrm{s} = 0.961$ (Planck Collaboration XIII 2016). All metallicities are defined with respect to the solar metallicity, set to $Z_\odot = 0.02$.

2.2 Binary evolution model

We consider binary evolution in the field, neglecting possible GW sources from N-body stellar dynamics in globular clusters or other formation channels (Rodriguez et al. 2015; Mapelli 2016; O'Leary, Meiron & Kocsis 2016), including Pop III stars (Kinugawa et al. 2014). We focus on the current standard picture of massive binary evolution and neglect alternate channels based on chemically homogeneous evolution (Mandel & de Mink 2016; Marchant et al. 2016). Throughout the paper, quantities refer to BH properties and we use superscript '$*$' to refer to properties of the progenitor stars in ambiguous cases (such as the mass).

As in Lamberts et al. (2016), we use the binary stellar evolution code (BSE; Hurley, Tout & Pols 2002), with modifications for massive binaries. Rapid binary population synthesis codes like BSE are based on prescriptions for the stellar evolution and interactions based on the initial masses and metallicity of the stars. Such codes allow for a computationally efficient exploration of a wide range of parameters, but can miss important effects in the stellar structure and mass transfer (Eldridge & Stanway 2016).

Currently, the main uncertainties in the evolution of massive binary stars are their mass-loss rates (especially for low-metallicity stars), the outcome of the common envelope interactions, the effect of SN kicks and the remnant masses. We use the metallicity-dependent prescription for the mass-loss rates from Belczynski et al. (2010a). We use the simplified prescription from Belczynski et al. (2008) for the remnant mass, which neglect details about the stellar structure (Eldridge & Tout 2004; Sukhbold et al. 2016). We use the model from Dominik et al. (2013) for the BH initial kicks, which are drawn from a Maxwellian distribution that peaks at 265 km s^{-1}. The kicks are then reduced according to the amount of material that falls back after core collapse (i.e. by a factor $M_\mathrm{BH}/M_\mathrm{NS} \simeq M_\mathrm{BH}/1.4\,M_\odot$, such that more massive BHs experience smaller kicks) consistent with the analysis by Mandel (2016). For example, a 14 $M_\odot$ BH (roughly the median mass of the BHs in our binaries) is given a typical kick of $\sim$25 km s^{-1}. This is lower than values quoted in Repetto, Davies & Sigurdsson (2012), based on the locations of low-mass X-ray binaries in the MW. The latter assume the binaries were formed in the mid-plane of the galaxy and find that kick velocities comparable with NS kicks are necessary in order to reach their current location. Based on our simulations, we find that most of the binaries are in the halo or the thick galactic disc. As such, their locations can be explained independently of natal kicks and solely based on the cosmological assembly of the Galaxy and its large-scale dynamics. For the common envelope mass transfer, we use the so-called α-formalism (Webbink 1984), using the common envelope efficiency $\alpha = 1$ and the envelope binding energy is determined according to the evolutionary stages of the stars. When common envelope occurs during the Hertzprung gap (between core hydrogen burning and shell hydrogen burning), we assume that a stellar merger occurs, as the boundary between the core and envelope is too smooth to stop the inspiral (Ivanova & Taam 2004, referred to as model B in Belczynski et al. 2007). Globally, we assume that half of the mass lost by the donor during Roche-lobe overflow is accreted by the secondary. Fig. 2 shows the resulting mean, minimal, and maximal mass of the primary BH as a function of the primary progenitor mass for $= 0.01, 0.1, 1\,Z_\odot$. In general, binary interactions lead to a wider range of possible BHs masses than might be expected from a single star of the same initial mass.

We create 13 different samples from the BSE model with metallicities logarithmically spaced between $Z = 0.005\,Z_\odot$ and $1.6\,Z_\odot$ ($Z_\odot \equiv 0.02$),[5] which are the limits currently allowed in BSE. For each metallicity, we build a statistical sample of binaries, with primary masses M_{1*} between 20 and 120 $M_\odot$ following a Kroupa IMF (Kroupa 2001). The secondary masses M_{2*} are drawn assuming that the mass ratios are uniformly distributed, and the initial period distribution is taken from Sana et al. (2012) (power law in log space with exponent $p = -0.55$). As (single) stars above 120 $M_\odot$ are likely subject to pair-instability supernova, which does not leave any remnant (Heger et al. 2003), we choose not to expand our upper limit. We begin with a thermal distribution for the eccentricities ($f(e) \propto e$), which favours high-eccentricity systems. While the initial conditions of the binary evolution (masses and orbital parameters) are somewhat uncertain, de Mink & Belczynski (2015) showed that these uncertainties only affect the final results by at most a factor of 2. We set the binary fraction to unity; all numbers can be directly rescaled to lower values. The number of binaries simulated with BSE depends on the metallicity, and is adjusted in order to ensure that our star particles are matched to a smooth distribution of BBHs. In practice, we require at least 3500 BBHs per metallicity bin, which requires an initial sample of approximately 30 000 binaries at $Z = 0.005\,Z_\odot$ but roughly 5×10^7 at the highest metallicity.

At most 8 per cent of the initial binaries result in BBHs (for the lowest metallicity). About two-thirds of the binaries have companions that are too low mass (initial $M_{2*} \lesssim 20\,M_\odot$) to allow the formation of a second BH. Among the massive enough binaries, about a third will undergo stellar mergers (see Fig. 1). This is consistent with the estimates of de Mink et al. (2014) that about 10 per cent of massive stars on the main sequence are merger products. Roughly another third of the binaries that would be massive enough to yield a BBH will instead be disrupted during the one of the supernova explosions; the remaining third will result in a BBH. At metallicity beyond $\simeq 0.3\,Z_\odot$, BBH creation is available to less than one per cent of stellar binaries due to mass-loss from stellar winds.

Fig. 3 shows the total mass $M_\mathrm{tot} = (M_1 + M_2)$ and orbital period P_orb at the formation of the BBH according to our binary evolution

[4] Whenever we refer to the simulation, we use the words star, particle, and star particle interchangeably.

[5] We use $Z = 5 \times 10^3, 10^{-2}, 1.6 \times 10^{-2}, 2.5 \times 10^{-2}, 4.0 \times 10^{-2}, 6.3 \times 10^{-2}$, 0.10, 0.16, 0.25, 0.40, 0.63, 1.0, 1.6 times the solar metallicity.

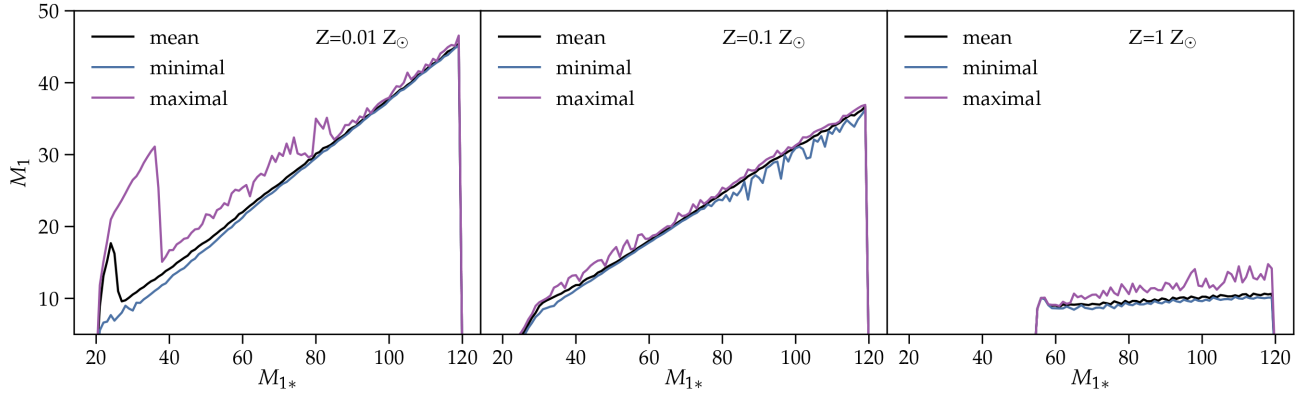

Figure 2. Mean (black) and extremal masses of the primary BH as a function of the primary progenitor mass for increasing metallicity for the binary evolution model presented here.

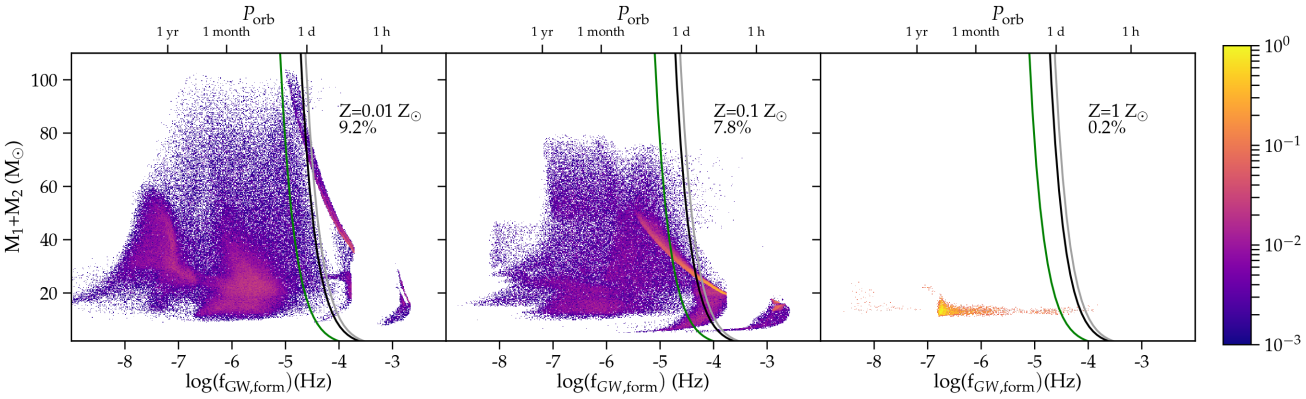

Figure 3. Properties of BBHs at their formation times for different stellar metallicities. We show the total binary masses ($M_1 + M_2$) versus initial orbital period ($P_{\rm orb}$) or equivalently the gravitational wave frequency of an equivalent circular orbit $f_{\rm GW}$ (the orbits are not necessarily circular, but this is intended only to guide the reader). The colours are normalized to the total number of BBH formed in each metallicity bin, while the percentage value shows the percentage of massive binaries that evolve into BBHs. The black/grey lines across the plot shows the maximal initial period for circular systems to be able to merge, assuming they formed at the beginning of the Universe or at $z = 1$, respectively. The green line shows the minimal period for a merger within a Hubble time for BBHs with initial eccentricity $e > 0.7$, which is the case for about 1 per cent of the systems at all metallicities. Most systems left of the black line cannot have merged by the present day.

model. Assuming circular orbits, we indicate the corresponding gravitational wave frequency (twice the value of the orbital frequency). These plots shows that BBH formation is rare at solar metallicity, and limited to $M_{\rm tot} \leq 30$, in agreement with Belczynski et al. (2016) and Eldridge & Stanway (2016). The lowest frequency systems stem from binaries that never interacted. At $Z \leq 0.3\,{\rm Z}_{\odot}$, BBH formation occurs for about 7 per cent of more massive binaries, but only the lowest metallicity model routinely produces binaries with $M_{\rm tot} > 60\,{\rm M}_{\odot}$, as stars at higher metallicities lose most of their mass in strong winds due to higher opacities in their atmosphere.

More specifically, for the lower metallicity models, several channels to BBH formation appear. The systems with the shortest initial orbit (or highest frequency) result from initial stars with $M_* \leq 50\,{\rm M}_{\odot}$, a stellar mass ratio q close to unity and a wide enough initial orbit to avoid stellar mergers during the common envelope phase. The narrow strip of binaries with orbits of order of a day typically have $M_2 \geq M_1$ and result from more massive stars with initial mass fractions close to unity. These systems have undergone important mass transfer from the primary to the secondary. The other binaries come from initially closer orbits, with stars with $0.3 \leq q \leq 0.8$ and $M_{1*} \leq 35\,{\rm M}_{\odot}$. Systems with periods of order a month or larger typically come from equal mass binaries at higher masses.

The main output of the BPS is a list of 3500 'sample' binaries for each metallicity. For each binary, we record its initial stellar masses and orbital properties, the formation time of the BBH $t_{\rm form}$ with respect to the formation of the progenitors and its masses and orbital properties. In the next section, we explain the gravitational wave properties of a given binary.

2.3 Gravitational wave emission

After the BBH is formed, the binary evolves only via gravitational wave radiation, gradually shortening the orbit. To assess the BBH population of the galaxy at any given point in time t, we first need to determine whether a binary with given properties has already merged. The time to coalescence is given by e.g. Maggiore (2008)

$$T_m = 9.829\,{\rm Myr} \left(\frac{T_0}{1\,{\rm hr}}\right)^{8/3} \left(\frac{{\rm M}_{\odot}}{M_1 + M_2}\right)^{2/3} \left(\frac{{\rm M}_{\odot}}{\mu}\right) F(e_0), \quad (1)$$

where μ is the reduced mass of the BBH, e_0 the initial eccentricity of the binary, and F a function depending on the orbital evolution of the system, which is equal to unity for circular binaries (see equation 4.137 in Maggiore (2008).

If the binary has not yet merged, its semimajor axis a and eccentricity e, which determine its GW emission, evolve according to Peters & Mathews (1963):

$$\frac{\mathrm{d}e}{\mathrm{d}t} = -\frac{304}{15}\frac{G^3\mu(M_1+M_2)^2}{c^5a^4}\frac{1}{(1-e^2)^{5/2}}\left(1+\frac{121}{304}e^2\right),$$
$$\frac{\mathrm{d}a}{\mathrm{d}t} = -\frac{64}{5}\frac{G^3\mu(M_1+M_2)^2}{c^5a^3}\frac{1}{(1-e^2)^{7/2}}\left(1+\frac{73}{24}e^2+\frac{37}{96}e^4\right). \quad (2)$$

For eccentric sources, GWs are emitted over a range of harmonics of the orbital frequency, while only the second harmonic emits for circular orbits. The total energy loss can be significantly higher than for circular orbits, resulting in faster inspirals. Even though many binaries are eccentric at birth, we find that the orbits are close to circular ($e < 0.15$) by the present day. As such, we include eccentricity for the orbital evolution, but compute the present-day GW emission assuming circular orbits. For circular orbits, the frequency and characteristic strain of the GW at a given distance d of the source are given by

$$f_{\mathrm{GW}} = \frac{1}{\pi}\sqrt{\frac{G(M_1+M_2)}{a^3}}, \quad (3)$$

$$h_{\mathrm{c}} = \left(\frac{32}{5}\right)^{1/2}\frac{(M_{\mathrm{c}}G)^{5/3}}{dc^4}\pi^{2/3}f_{\mathrm{GW}}^{7/6}, \quad (4)$$

where the chirp mass is given by $M_{\mathrm{c}} = (M_1M_2)^{3/5}(M_1+M_2)^{-1/5}$.

2.4 From an MW model to GW emission

The core of this paper is the combination of a binary population synthesis model (Section 2.2) with a cosmological model for a MW-mass galaxy (Section 2.1) and its star formation history as a function of localization and metallicity to determine the GW emission (Section 2.3). Here, we describe how these three aspects are combined during post-processing of the simulation.

We first bin the star particles from the **m12i** simulation into the same 13 metallicity bins as our BPS model. Stars with metallicity below/above the range covered in the BPS model are assigned to the first/last bin. Each star is then randomly assigned a binary from the BPS model at the corresponding metallicity. This effectively associates BH masses M_1, M_2, an orbital period P_0 and eccentricity e_0 of the BBH at formation with each star. We also keep track of the formation time of the BBH with respect to the formation of the progenitor stars t_{form}.

To obtain the present-day distribution of BBH, we determine the time $\mathrm{d}t = t_H - (t_{\mathrm{form}} + t_*)$ over which to evolve the binary in order to reach t_H, the present-day age of the universe. We evolve all the BBHs forward during $\mathrm{d}t$ according to equation (2) and their initial orbits and masses. For each BBH, we then have the present-day orbital parameters if it has not yet merged (from GW evolution); and spatial localization (from the simulation) and can determine its gravitational wave properties and possibilities for electromagnetic detection.

In this method, we have assumed that each star particle can be uniquely associated with a single BBH. In practice, the star particles have a mass $\simeq$7000 $\mathrm{M}_\odot$ and represent an IMF-averaged group of stars. From the Kroupa IMF, we find that there are about 12 binaries with $M_{1*} \geq 20$ in such a star particle. For each metallicity, we can determine the expected number of BBHs according to the fraction of massive stars that effectively turn into a BBH (see percentages in Fig. 3). Effectively, we find that star particles with $0.025 \leq Z \leq 0.4$ typically form one BBH, stars with lower metallicity create between 1 and 2, and stars with higher metallicity rarely make BBHs. As such, we weigh all of our mock statistical BBHs with the expectation value of the number of BBH associated with an IMF-averaged stellar population of the same mass, age, and metallicity as the simulation star particle. We perform a polynomial fit of the fraction of BBHs as a function of metallicity and use this to extrapolate the probability of producing a BBH for systems beyond our initial metallicity range.[6] This weighting is accounted for in all the results presented here.

Although we include BH natal kicks to determine the initial orbits of the BBH in our BPS model, we do not assign these same kicks to our particles and the location of the BH is set by the location of the star particle they stem from. As we discuss in Section 5, we estimate that this approximation does not impact the main results of our study.

3 BHs IN A MW-MASS GALAXY

Fig. 4 shows the distribution of formation time and metallicity of all the stars within 300 kpc (top) and the subset of stars that are UMBHs at $z = 0$ (middle) as well as systems that have already merged (MBBH, bottom). The star formation extends from very early times to the present day, and is consistent with the global peak of star formation between 10 and 4 Gyr ago (Madau & Dickinson 2014). While the stellar metallicity globally increases over time, the scatter is important at all ages. The BPS model (Section 2.2) highlighted that the formation of BBHs very strongly depends on metallicity. While the bulk of recent star formation is significantly supersolar, about a per cent of the recent star formation is low enough metallicity to potentially allow BBH formation. Recent star formation in **m12i** occurs at slightly higher metallicities than observations suggest is the case in the MW (Mackereth et al. 2017). However, we emphasize that the drop-off in BBH formation with increasing metallicity is so steep that our predictions would only be marginally impacted by reducing the metallicity of late-time star formation by a factor of 2. However, this difference does somewhat depress the number of BBHs in the disc of our model MW. The data for this plot is provided at https://fire.northwestern.edu/data/. We also provide the list of BBHs and their masses, present-day gravitational wave frequency and position in the galaxy.

The middle plot shows the progenitor stars of the UMBH population. The distribution is very limited above $Z \simeq 3\,\mathrm{Z}_\odot$, because BBH formation becomes extremely rare (see Fig. 3). This means that in MW-mass galaxies, the bulk of the massive stars formed recently are unable to form BBHs. Star formation over the past 500 Myr accounts for 3 per cent of the total stellar mass but only 0.3 per cent of the mass in BH binaries. Most of the currently present BBHs come from stars formed 8–10 Gyr ago (between $z = 1$ and $z = 2$), when low-metallicity star formation was the strongest.

The distribution of progenitor stars of MBBH is shown in the bottom panel. Globally, the systems that have already merged by $z = 0$ originate as lower metallicity stars, and thus trace older star formation. This confirms the results presented in Lamberts et al. (2016). The upper limit on the metallicity is around $Z \simeq 0.2\,\mathrm{Z}_\odot$ in the BPS model presented here, and the cut-off is even more drastic than for the unmerged systems. This is because the few BBHs that are formed at higher metallicity typically have wide orbits and low chirp masses due to differences that arise during the course of stellar

[6] Due to the strong dependence on metallicity (as shown in Fig. 3), this extrapolation produces a negligible number of additional BBHs and therefore has a minimal impact on our results.

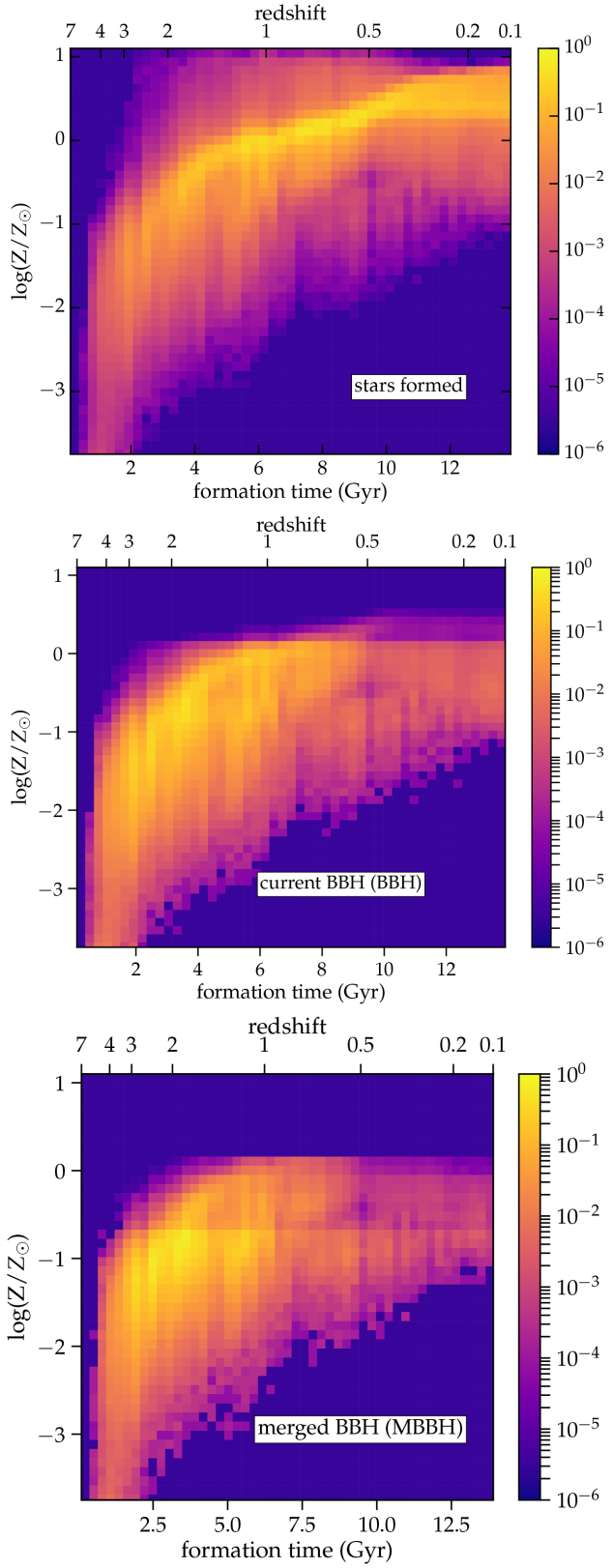

Figure 4. Distribution of the formation time and metallicity of all the stars within 300 kpc of the centre of the galaxy in the simulation (top), those stars that are progenitors of the currently unmerged-BBHs (middle) and the progenitors of the BBHs that have already merged (bottom). All distributions are normalized to unity.

evolution, implying that they will never merge within a Hubble time (see Fig. 3, and also delay time distributions in Belczynski et al. 2008; Dominik et al. 2012; Lamberts et al. 2016). The exact cut-off is strongly dependent on the details of the BPS model, such as the mass-loss through stellar winds, BH natal kicks and the outcome of common envelope evolution, and will likely be revised as our understanding of massive stellar binaries improves. However, an upper limit on the metallicity is likely to persist. Models accounting for strong mixing within the stars (Mandel & de Mink 2016; Marchant et al. 2016) are also limited to low-metallicity progenitors and are likely to stem from the same progenitor population.

These plots show that UBBH/MBBH in MW-mass galaxies stem from a different population than most of the stars. As such, we can expect them to also have a different spatial distribution. Fig. 5 shows maps of the distribution of stellar mass (top) and mass in (merged and unmerged) BBH for a MW-mass galaxy viewed face-on (left) and edge-on (right). The stellar mass distribution shows a zoomed-out view of a spiral galaxy with a central bulge and bright disc. The halo, which is more scarcely populated, extends to about 40 kpc. Beyond, we find satellites and streams due to infalling satellites. In comparison, the BBH distribution is much less concentrated in the bulge and disc; instead, the halo is much more populated. Additionally, the satellites and streams overproduce BBHs with respect to their stellar content. Satellites are low-mass galaxies (see Wetzel et al. 2016 for a full description) with low-metallicity star formation. Accordingly, these are prime sites for BBH production and mergers (Lamberts et al. 2016; Mapelli et al. 2017; Schneider et al. 2017; Elbert et al. 2018).

Fig. 6 provides a quantitative description of the spatial distribution of the BHs in a MW-mass galaxy. Globally, the BBHs are preferentially on the outskirts of the galaxy. The effect is even stronger for the merged systems. About 60 per cent of the systems are located more than 10 kpc from the centre of the galaxy, while 95 per cent of the stellar mass is concentrated within that distance. The right-hand panel plots BBH counts as a function of distance above or below the plane of the disc of the galaxy. Roughly 50 per cent of the BBHs are located at least 3 kpc above or below the disc mid-plane. The sudden increases in the cumulative distribution function at radii beyond 100 kpc indicate BBHs in satellite galaxies, which effectively contribute between 5 and 10 per cent of the systems. When considering the mass distribution of systems, we find that the respective dominance of the stellar halo and satellites is even stronger for the systems with total masses above 50 $M_\odot$, 10 per cent of which lie beyond 50 kpc in satellites and streams, even though the latter contribute less than 1 per cent of the total stellar mass.

Fig. 7 shows the distribution of merged and unmerged systems as a function of total mass of the BBH (left) and metallicity of the progenitor star (right). The total number of systems is shown with the solid lines. Out of a stellar mass of 7.3×10^{10} $M_\odot$ within 300 kpc, we find 6.8×10^5 merged BBH systems and 1.2×10^6 unmerged systems. Out of the total current stellar mass, there is a total of 5.3×10^7 $M_\odot$ in BHs from binary systems (merged or not merged). Assuming that the current stellar mass traces the total star formation we find that 0.07 per cent of the stellar mass in a MW-mass galaxy turns into a BH binary. We remind the reader that we do not account for BHs with other companions or that have been kicked out of the initial binary. colorblack[7] We provide an estimate of the total number of BHs in a MW-mass galaxy in Section 5.

[7]We note that some of the mass will be radiated away through gravitational waves as the binaries merge.

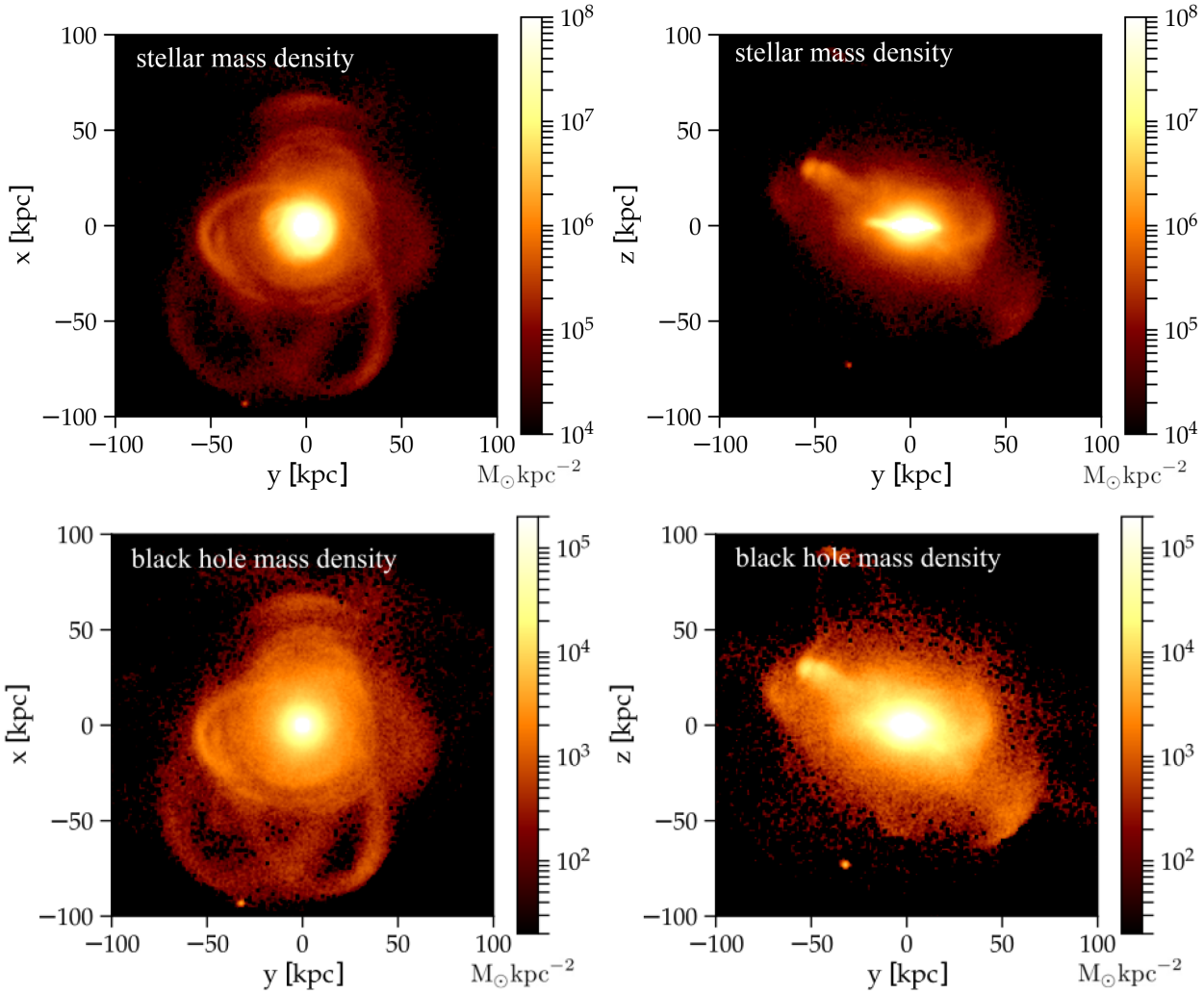

Figure 5. Maps of the projected stellar mass density (top) and the isolated BH mass density (merged and unmerged) (bottom) for a face-on (left) and edge-on view (right). The two rows show different absolute values (in units of Solar mass per kpc^2), but the dynamic range of the colours is identical, allowing for comparison between the two spatial distributions. The upper row represents the total stellar mass and is not a mock observation, which would prominently show young stars and include dust attenuation. At smaller scales, galactic components such as the bulge and thin and thick disc are more prominent. The halo, streams, and satellite galaxies are overrepresented in the IBH maps owing to their lower metallicities, though we note that supernovae kicks, which we do not include in this work, may smear BBHs relative to the stellar streams and potentially eject them from the satellites. As described in Wetzel et al. (2016), the cosmological simulation produces a realistic distribution of the MW satellites down to a stellar mass of $10^5\,M_\odot$.

The mean (median) mass is 28.9 (25.4) $M_\odot$ for the MBBHs. For the UBBHs, the mean (median) total mass is 28.1 (24.7) $M_\odot$ for UBBHs. This is because most of the BBHs come from progenitors with $0.03 \geq Z/Z_\odot \geq 0.2$, where systems with wider obits, which have not merged yet, have more massive BHs (see Fig. 3). Both for the merged and unmerged systems, massive binaries with total masses above 50 $M_\odot$ make up about 10 per cent of the systems and systems above 80 $M_\odot$ make up less than 1 per cent of the systems.

The mean (median) metallicity of the progenitor stars is 0.13 (0.1) $Z_\odot$ for the MBBHs and 0.25 (0.14) $Z_\odot$ for the UBBHs. While extremely low-metallicity progenitors ($Z < 0.01\,Z_\odot$) are prime candidates for BBH formation (see Section 2.2), they only contribute about 5 per cent of the systems in MW-mass galaxies. Conversely, progenitors formed with $Z > 0.3\,Z_\odot$ contribute about 30 per cent of the unmerged systems and 10 per cent of the merged systems. In our model, progenitors with supersolar metallicity contribute less than 1 per cent of the formed BBHs. The mean and median values are summarized in Table 1.

The shaded area in both histograms shows the number of systems formed outside of the main galaxy. Stars are considered to have formed ex situ if their initial distance to the galactic centre was more than 30 kpc (where 'galactic centre' refers to the centre of the main progenitor of the $z = 0$ galaxy, at the time the stars formed). Such systems have either merged into the galaxy by now (and are present in the bulge/halo), are in the process of being merged (and are present in streams) or are still present in the dwarf galaxy where they formed (and are now in satellites). In our MW model, less than 5 per cent of the currently present stellar mass is formed ex situ (Anglés-Alcázar et al. 2017; Sanderson et al. 2017). In comparison, we find that more than a third of the BHs (merged and not merged) come from ex situ formation. For total BBH masses above 60 $M_\odot$, only 40 per cent of the systems were initially formed within the main galaxy. This is because, more than 90 per cent of the stellar mass with $Z < 0.01\,Z_\odot$ originates outside the main galaxy, as does about half of the stellar mass with $Z < 0.1\,Z_\odot$.

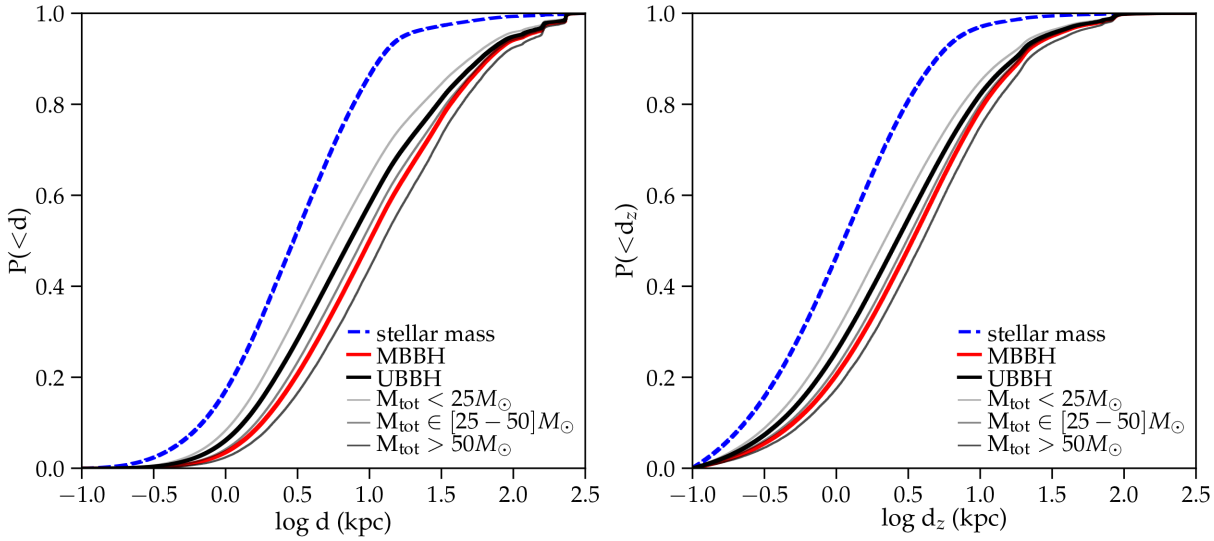

Figure 6. Cumulative distribution function of the number of merged black holes (MBBH, red) and unmerged black holes (UBBH, black) as a function of distance to the galactic centre (left) and vertical distance away from the plane of the galaxy (right). The distribution of the stellar mass is shown as a blue dashed line for comparison. For the merged systems, we distinguish different mass ranges with different grey scales. More massive binaries require lower metallicity and are further biased towards the halo and streams and satellites.

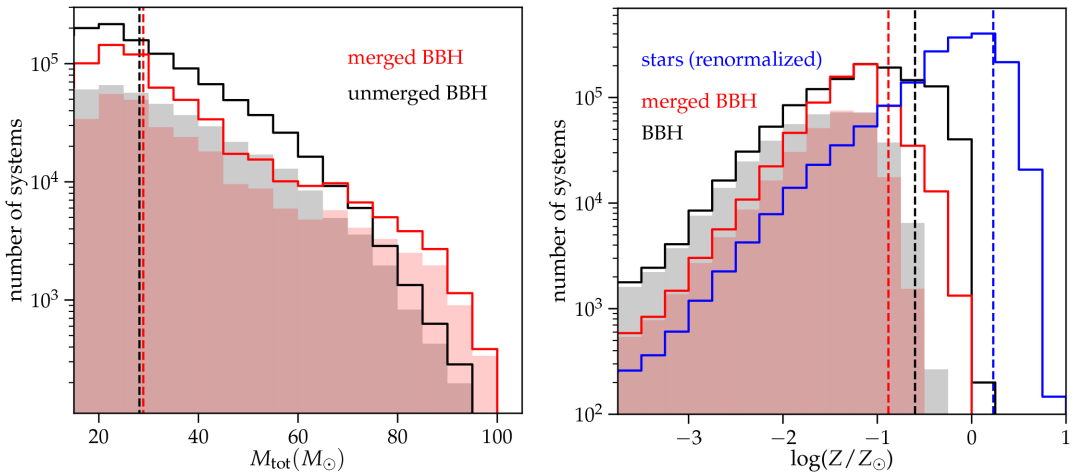

Figure 7. Number of merged BBH (MBBH, red) and unmerged BBH (MBBH, black) as a function of total mass (left) and progenitor metallicity (right). The vertical dashed lines show the mean masses and metallicity of the merged and unmerged systems. The lines show the total number of systems, while the shaded areas only represent systems formed outside of the main galaxy. The blue line on the right shows the stellar mass (divided by $5\times10^4\,\mathrm{M}_\odot$) for comparison. Above $Z > 0.01\,\mathrm{Z}_\odot$, the vast majority of the stars come from *in situ* formation (not shown here). The comparison between stars and BBH progenitors clearly shows that there are more total stars at high metallicity, but more efficient BBH formation at lower metallicity, producing the 'peak' at $Z \simeq 0.1\,\mathrm{Z}_\odot$.

Table 1. Summary of the mean and median properties of the merged and unmerged systems.

	$Z/\mathrm{Z}_\odot$		$M/\mathrm{M}_\odot$	
	Merged	Unmerged	Merged	Unmerged
Mean	0.15	0.26	26.5	28.4
Median	0.11	0.20	22.5	24.5

According to our combination of a cosmological model for a MW-mass galaxy and binary population synthesis, we find about 2 million BH systems stemming from binary interactions, a third of which have merged by now. In the following section, we describe the prospects of detecting these single and BBHs with gravitational waves or electromagnetic signatures.

4 OBSERVATIONAL PERSPECTIVES

Regardless of the detection method, the spatial distribution of the BBHs is a key in determining observational survey strategies. Fig. 8 shows the distance to the sources (MBBHs and UBBHs) with respect to the Sun, i.e. at an arbitrary point along the Solar Circle: on the disc mid-plane and 8 kpc from the centre of the galaxy. About 300 merged systems and 500 binaries are present within a kpc. Unfortunately, the majority of both the merged and unmerged systems are located beyond 10 kpc. Most of those are in the galactic halo, off the plane of the disc (see Fig. 6). Finding these sources would require the monitoring of a large fraction of the sky with a deep survey.

Extragalactic mergers of BBH BHs have been detected with gravitational waves (Abbott et al. 2016b) for $z < 0.2$. The local

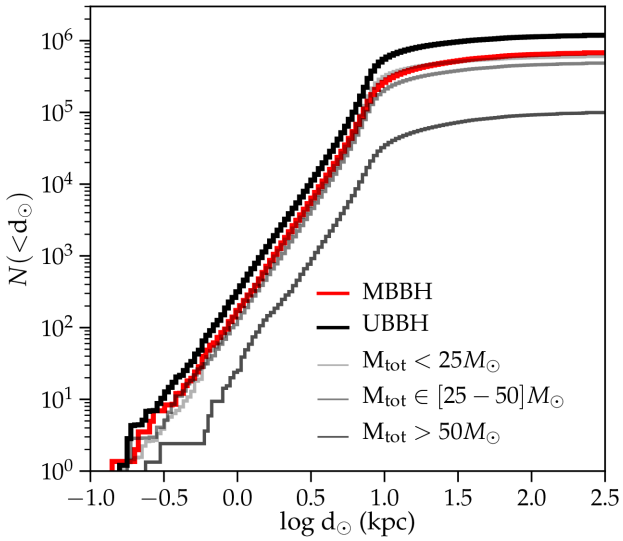

Figure 8. Number of predicted merged (red) and unmerged (black) BBH systems within a given distance of a randomly chosen point on the Solar Circle (i.e. 8 kpc from the galaxy centre in the plane of the disc.).

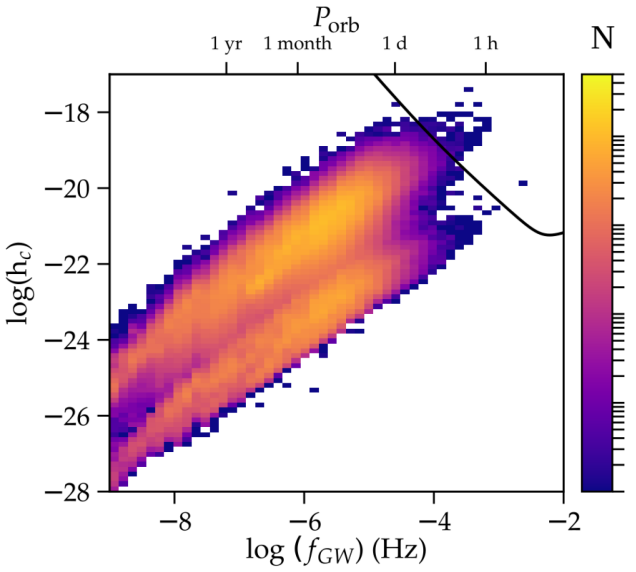

Figure 9. Characteristic strain and GW frequency of the BBHs in our simulation assuming 4 yr of observations. The black line in the upper right corner shows the current expected sensitivity curve of the *LISA* mission – only binaries above the line may be detectable. The colour shows the number of systems in each bin.

BBH merger rate inferred by LIGO is 12-213 $\mathrm{Gpc^{-3}\,yr^{-1}}$ (Abbott et al. 2017c). Assuming 5×10^{-3} MW-mass galaxies per comoving $\mathrm{Mpc^{-3}}$ (Baldry, Glazebrook & Driver 2008), this yields a galactic merger rate $6 \times 10^{-6} < R_{\rm MW} < 10^{-4}\,\mathrm{yr^{-1}}$, assuming all mergers occur in MW-mass galaxies. This makes a BBH merger very unlikely in the MW (Abbott et al. 2016c). At much lower frequencies, *LISA* is currently the only planned GW detector that may detect BBHs before they merge. *LISA* will be able to detect cosmological BBHs just a few years before they merge within the LIGO band (Sesana 2016), and it may also be able to detect BBHs in the MW or its nearby satellites thousands of years before they merge (Belczynski et al. 2010b). Given the negligible likelihood of a merger occurring within the MW itself, we focus here on the latter possibility.

Fig. 9 shows the gravitational wave frequency and characteristic strain expected from each binary after 4 yr of observations in our model galaxy (equations 4). It shows two distinct populations, with similar frequency distributions but different median values for the strain. The upper population is exclusively composed of binaries within the galaxy, while the lower group is composed of binaries within satellites. The 'loudest' binaries ($h_c > 10^{-20}$) have total masses above 40 $\mathrm{M_\odot}$ and are all located within 30 kpc of the Sun, mostly within the disc. The black line in the upper left corner represents the expected noise curve for *LISA* (Klein et al. 2016; Amaro-Seoane et al. 2017).

We find that (for our specific binary evolution model) about 25 binaries will be detectable with a signal-to-noise ratio above five after 4 yr of observations. In our method, binary properties are drawn probabilistically (in Monte Carlo fashion) for each star particle according to its age and metallicity. We also vary the localization of the Sun along an annulus 8 kpc away from the Galactic centre. The global properties of the binaries are identical for different realizations of the model and different positions of the Sun. We find similar results for **m12b**. **m12c** predicts roughly twice as many detectable BBHs because it is much more compact, decreasing the typical distance of binaries in the main galaxy. We caution that **m12c** is more compact than the MW, however (Porcel et al. 1998; Garrison-Kimmel et al. 2017). The lowest frequency systems correspond to frequencies probed by pulsar timing arrays, but the corresponding strains are almost 10 orders of magnitude below the current detection limit and will remain completely undetectable for the foreseeable future with the current methods.

The population represented in Fig. 9 results from a convolution between the star formation history and spatial structure of the galaxy and massive binary evolution. As shown in Figs 3 and 7, most of the binaries result from progenitor stars with $Z \simeq 0.2\,\mathrm{Z_\odot}$ and had an initial frequency $f_{\rm GW} < 10^{-5}$ (orbit longer than a day) and quasi-circular orbits. The high-frequency binaries as well as most of the low-metallicity binaries shown in Fig. 3 have merged by now. The highest frequency systems ($f_{\rm GW} > 10^{-4}$) typically have a total mass below 25 $\mathrm{M_\odot}$ and come from progenitors with metallicity $Z \simeq 0.3\,\mathrm{Z_\odot}$.

The detection of stellar BHs without stellar companions, whether they are single BHs or BBHs, is strongly limited as such systems do not emit any electromagnetic radiation. The current strongest indications for the presence of BHs without stellar companions in the MW come from microlensing events with inferred lens masses up to $\simeq$10 $\mathrm{M_\odot}$ and no detectable electromagnetic counterpart (Wyrzykowski et al. 2016). Massive lenses lead to months-to-year long lensing events. Distinguishing between binaries with a short orbital period or single sources would be impossible making the merged systems, unmerged systems and BHs formed through any other channel (see Fig. 1) indistinguishable. Without additional information on the distance to the lensed source, it is impossible to break the degeneracy between the mass of the lens and its distance (Agol et al. 2002). As such, BH candidates can only be identified in a probabilistic sense. Surveys targeting dense regions like the bulge of the galaxy are the best suited for this type of analysis (Wyrzykowski et al. 2016). When the distance to the source and lens are known through microlensing parallax, the mass of the lens can be determined. Surveys of the Magellanic Clouds or other nearby galaxies are the best suited for this type of search (Wyrzykowski et al. 2011; Mirhosseini & Moniez 2017), although those events would be very rare due to the small density of the lenses. If our

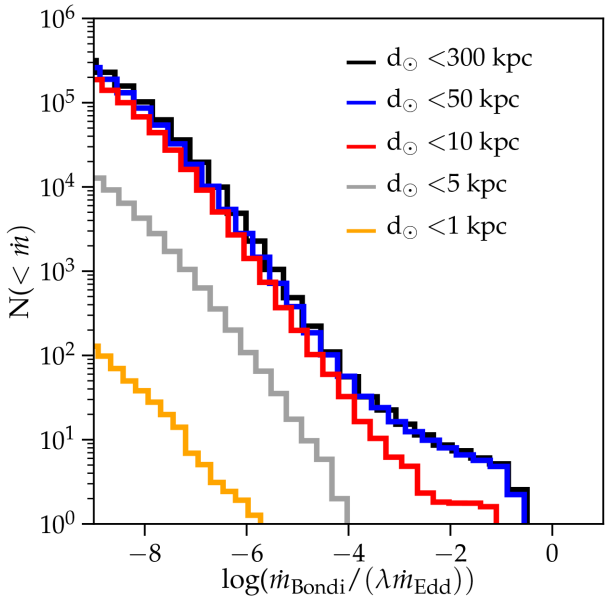

Figure 10. Cumulative distribution function of the Bondi–Hoyle accretion rate of the ambient gas by merged and unmerged BBHs normalized to the Eddington accretion rate and the Bondi–Hoyle accretion efficiency λ. Different colours indicate different distance cuts.

conclusions hold for the global distribution of BH in the MW (see Fig. 1 for all the BHs not considered here), a long-term survey of the Magellanic Clouds or M31 may be the best option to find single BHs.

Faint X-ray and radio emission may be detected if BHs are accreting surrounding gas (Maccarone 2005). Fig. 10 provides the Bondi–Hoyle accretion rate $\dot{m}_{\rm Bondi}$, with respect to the Eddington accretion rate for all our BHs. The Bondi–Hoyle accretion rate is given by

$$\dot{m}_{\rm Bondi} = \lambda 4\pi (GM)^2 \rho (v^2 + c_{\rm s}^2)^{-3/2}, \quad (5)$$

where v is the velocity of the BH with respect to the ambient gas and $c_{\rm s}$ and ρ are the sound speed and density of the accreted gas. The parameter λ is an 'efficiency' factor that represents our ignorance on detailed accretion physics. Observational estimates suggest $\lambda = 10^{-2}$–10^{-3} based on accretion on to NSs (Perna et al. 2003). Based on these values of the accretion efficiency, most BH systems are expected to accrete at less than 10^{-6} times the Eddington accretion rate. This is because only a small fraction of our BHs are located in the disc and bulge, close enough to dense molecular clouds, where accretion would be large. Moreover, the BHs we consider stem from old stars, which have high proper velocities with respect to the gas. Isolated BHs kicked out of binary systems are likely to have a similarly high velocity, and small accretion rate. The systems with the highest accretions rates are located in a star-forming satellite galaxy. The radiative properties of the accreting BHs dependent on the geometry, cooling properties, and radiative mechanisms of the accretion flow, which are highly uncertain at these low accretion rates, especially in binary BHs. But if λ is high in these systems, as many about 10 merged or unmerged BBH systems, mostly moving through dense molecular clouds in the inner disc or star forming satellites, could be accreting at sufficiently large rates to be detectable with all-sky X-ray surveys. Around the MW, the Magellanic Clouds are the only known satellites still actively forming stars.

5 DISCUSSION

5.1 An improved MW model

The unique combination of a high-resolution cosmological simulation of an MW-mass galaxy and a binary population synthesis model allows us to predict the number of unmerged BBHs and merged BBHs in the MW, as well as their mass distribution and localization. From there, we can determine possible detections, with electromagnetic telescopes or gravitational wave detectors.

Our MW model is based on a cosmological simulation of an MW-mass galaxy down to $z = 0$ (Wetzel et al. 2016), with a mass resolution of $\simeq$7000 M$_\odot$. We find that the number, mass distribution and spatial distribution of the merged BBHs are nearly identical in a simulation of the same galaxy with a factor of 8 fewer particles (mass resolution of $\simeq$56 000 M$_\odot$). In contrast, the unmerged BBHs are 15 per cent more numerous in the lower resolution simulation, due to somewhat higher star formation after $z \simeq 1.5$. This results into more systems from progenitors with $Z > 0.1\,Z_\odot$, and a slightly lower mean mass for the BBH systems. The spatial distribution of the BHs is the same in both cases, aside from the satellites, which produce fewer BH in the lower-resolution simulation. Altogether, this suggests our results are not strongly sensitive to the resolution of the simulation.

More importantly, the simulation provides a fully cosmological model for the formation of a MW-mass galaxy, self-consistently modelling its stellar disc, satellite population, and stellar halo, each with cosmologically driven formation histories and self-consistent metal enrichment. This is a significant improvement over previous estimates of the population in the MW. The left-hand panel of Fig. 11 compares the star formation rate as a function of time and metallicity in the simulation, versus other models that are used to compute the binary population in the MW. Most models assume a constant star formation rate at Solar metallicity (straight monochromatic lines in Fig. 11) in the disc and bulge, if the latter is included at all. When present, the halo is assumed to come from a single star burst at $Z = 0.1\,Z_\odot$ (Voss & Tauris 2003; Belczynski et al. 2010b; Ruiter et al. 2010; Liu & Zhang 2014). All these models neglect supersolar metallicity star formation. Although this does not impact BBH formation, it may impact the formation of binary NSs and/or WDs (Nelemans et al. 2001; Ruiter et al. 2010). Only Mennekens & Vanbeveren (2014) include time-variable, metallicity-dependent star formation (coloured squares), although their model globally overpredicts early star formation and underestimates the variation in the mean metallicity over time compared to observational constraints in MW-mass galaxies (e.g. Behroozi, Wechsler & Conroy 2013). None of the models in the literature include scatter in the metallicity at a given time, while the dashed lines (and also Fig. 4) and observations (Garcia Perez et al. 2018) show that there is a typical range of about a dex between the highest and lowest metallicity at a given time. This is crucial as the lowest metallicity systems most significantly contribute to the formation of BBHs.

Models in the literature also neglect the crucial impact of galactic mergers. In Fig. 7, we have shown that about a third of the BBHs present in the MW come from progenitors formed in a satellite galaxy. At the highest masses, more than 60 per cent of the BBHs comes from ex situ formation. This is somewhat different from the findings of Chakrabarti et al. (2017) who predict that most of the progenitors of BBH mergers come from the outer disc of massive galaxies. Neglecting galactic mergers underestimates the global BBH population, specifically high-mass binaries and binaries in the galactic halo.

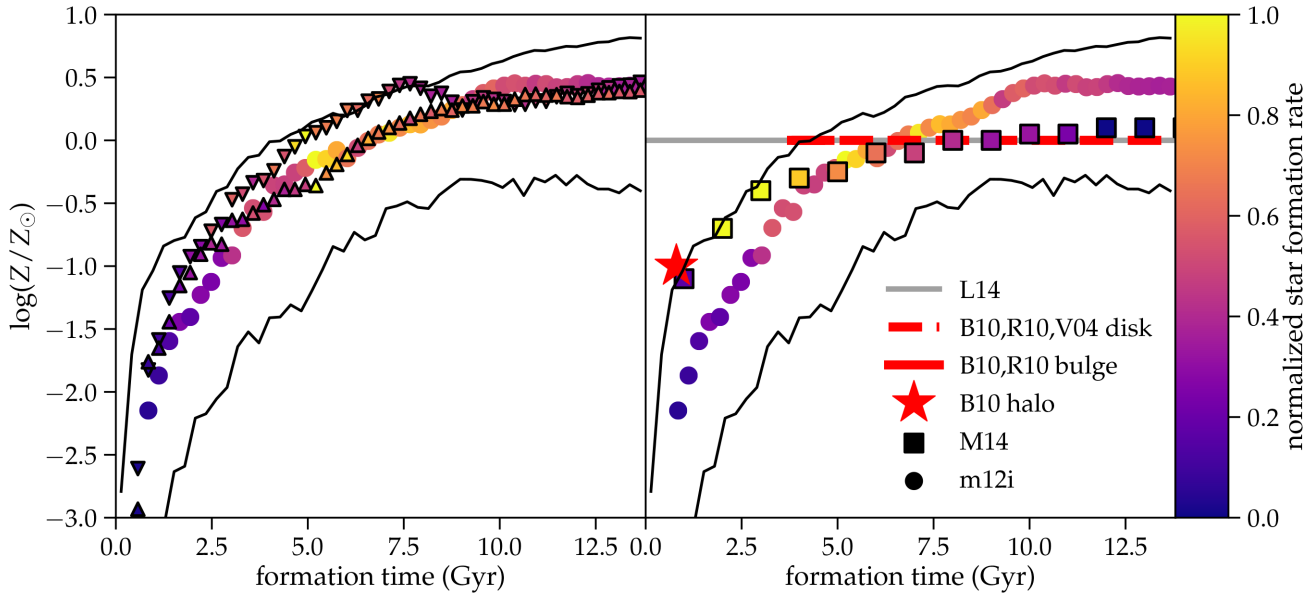

Figure 11. Comparison of the star formation rate as a function of metallicity and time used in the **m12i** simulation compared to other simulations of MW-type galaxies (left) from the FIRE project and previous models for the MW used to derive BH populations in the Galaxy (right). In both plots, the circles show the median values in the **m12i** simulation, colour coded by their relative star formation rate (SFR(t, Z)/max SFR) and the black lines show the 95 per cent scatter in metallicity for stars forming at the same time. On the left plot, monochromatic lines show models that assume a constant star formation rate (e.g. Voss & Tauris 2003; Ruiter et al. 2010; Belczynski et al. 2010b; Liu & Zhang 2014), while coloured points are shaded by the relative star formation rate at a given time (e.g. Mennekens & Vanbeveren 2014). Bursts of star formation are shown with stars symbols. On the right plot, we show the **m12b** simulation with inverted triangles and **m12c** simulation with triangles.

Belczynski et al. (2010b) assume that stars form at solar metallicity over the past 10 Gyr with a small contribution from the bulge and halo (at $Z = 0.1\,Z_\odot$). In contrast, the simulation shows that the majority of stars formed during the last 7 Gyr have a super-solar metallicity, and are unavailable to BBH formation. On the other hand, they neglect most of the star formation between $z = 1.5$ and 3, where we predict the majority of the BBHs originate (see Fig. 4). This may explain why their model B (which is similar to our BPS model) predicts about half as many binaries as our model, even though the assumptions on the binary evolution are very similar. They also neglect the contribution from ex situ stars, effectively missing 40 per cent of the binaries. We also predict more *LISA* detections, because, on average, our binaries stem from more metal-poor stars and produce more massive BHs.

We also show the star formation history of two other simulations of MW-mass galaxies run with the same resolution and physics (right-hand panel of Fig. 11). The **m12b** simulation has a 27 per cent higher present-day stellar mass than **m12i**, but produces fewer BHs. This is because most of its star formation is at too high metallicity to significantly produce BBHs (see inverted triangles in Fig. 11). **m12c**, meanwhile, has 7 per cent less present-day stellar mass, but also produces 15 (13) per cent fewer merged (unmerged) BBHs. This is because its low-metallicity star formation around $z \simeq 2$ is lower than in our reference simulation. The global properties (mass, progenitor metallicity and spatial distribution) of the BHs are similar in the three simulations. The comparison with different MW-mass galaxies highlights the robustness of our calculation, and indicates that our simulation is a reliable representation of the MW galaxy, even though it is not an exact reproduction. The comparison also shows that although the present-day stellar mass provides a first indication of the BBH content of a galaxy, the details of its star formation history and more specifically its metallicity can have an important effect.

Our host galaxy has a higher present-day star formation rate than the MW. As recent star formation has a limited contribution to BBH formation (see Fig. 4), we do not expect this to influence the quality of our MW model. Although the global properties of the satellites are consistent with observations (Wetzel et al. 2016), the simulation does not show a massive satellite like the Large Magellanic Cloud. The latter still presents star formation with $Z \simeq 0.25\,Z_\odot$ (Harris & Zaritsky 2009) and is thus a prime candidate for BBH formation. As such, our estimate of the number of UBBH and MBBH within 300 kpc is likely a lower limit.

5.2 Pathways towards detections

The accurate spatial model in our fully cosmological simulation, with respect to simplified disc and halo models, allows us to provide some predictions of the detectability of the sources with electromagnetic or gravitational signatures. Although BH natal kicks are included in our binary evolution model, we do not model the impact of BH kicks on the location and proper motion of the BHs in the galaxy simulation. BHs kicks are assumed to be smaller than NS kicks, due to material falling back. As we are specifically focusing on BBHs surviving SN kicks, we are biased towards the BBHs with small natal kicks (otherwise the binary would have been disrupted). Additionally, most of our systems are found in the stellar halo, which is dominated by random motions, where BH natal kicks are likely to have a limited impact of the statistical properties of the total BBH distribution. Systems formed in the disc may be kicked into the halo, especially if the kicks occur before most the mass of the host galaxy is accreted ($z \lesssim 3$). For systems formed in satellite galaxies, kicks may be powerful enough to escape the shallow potential well of the dwarf galaxy, but it is unlikely that they would be able to escape the potential of the main host. As a result, the distribution of ex situ systems may be more randomized, and BBHs may

not closely trace stellar streams and satellites. Overall, we expect most of the merged and unmerged BBHs to be in the galactic halo, and we argue that this result is robust to our assumption that BBHs trace the location of their parent star particles.

The prospects for detecting BHs without stellar companions remain limited. Still, with a refined model of the star formation history in the MW, non-detections with X-ray, radio and microlensing surveys will put constraints on binary evolution models. Conversely, a much higher number of detected systems will be equally constraining, and may inform us of additional BBH formation channels (Rodriguez et al. 2015; Marchant et al. 2016). Our understanding of massive binary evolution is still very uncertain, especially the modelling of stellar mass-loss through different evolutionary phases, the properties of common-envelope mass transfer, and supernova kicks. Specifically, we have assumed that common envelope interactions during the Hertzprung gap result in stellar mergers, which may underestimate the BBH production rate. Conversely, we assume the BH natal kicks are reduced with respect to NS natal kicks, which may overestimate the number of systems surviving both supernova explosions. As our work highlights the importance of improved galactic models, we do not explore the wide parameter space of current binary models. The different BBH merger rates predicted by Mapelli et al. (2017) show how different binary evolution models will eventually be ruled in or out by observational data, provided appropriate models are used for the star formation.

Based on our assumptions for binary evolution, we predict that *LISA* will detect about 25 BBHs within the MW halo. The frequency of these systems will not vary over the duration of the *LISA* mission, which means that the measured chirp mass will be degenerate with the distance of the system (see equation 4) and discerning it from a closer NS binary may not be possible. While certain aspects of binary evolution are likely to be revised, we emphasize that the BBH predictions of our model are somewhat on the high end (see a discussion in Lamberts et al. 2016) and that fine-tunning it in order to produce more galactic BBHs may overproduce the observed BH merger rate (Abbott et al. 2017c). Unless a mechanism allows for the formation of BBHs at close to solar metallicity, BBHs are strongly biased towards the galactic halo, which strongly reduces their GW signal on Earth relative to disc populations. Even a single detection with accurate localization will provide information on the binary evolution mechanism and the conditions of its formation.

We find that less than a million BBHs have merged in the MW by the present day. Focusing on the mergers within the last 2 Gyr, we find a merger rate of $\simeq 10^{-5}$ yr^{-1}. Our model, which assumes a binary fraction of unity, is on the higher end of the measured rate. We find the mean mass of the systems to be 29 $M_\odot$, which is in line with the announced detections (Abbott et al. 2016a; 2017a,b,c). We find that sources with $M_{\rm tot} > 50\,M_\odot$ represent 8 per cent of the merged systems, meaning there could be roughly 40 000 such BBHs in our Galaxy. The progenitors of these systems likely formed in a satellite galaxy and are now present in the halo. Similarly to Lamberts et al. (2016), we find that mergers in MW-mass galaxies primarily stem from progenitors with $Z \simeq 0.1\,Z_\odot$.

Initial studies predicted roughly 10^8 BH in the MW (single and binary), based on stellar evolution models (Shapiro & Teukolsky 1983; van den Heuvel 1992) and yields from massive stars (Samland 1998). Based on metallicity-dependent star formation models of galaxies of all masses, Elbert et al. (2018) predict $\simeq 10^8$ BHs in the MW, with 10 per cent of them above 30 $M_\odot$. Our model predicts about a million BBHs and less than a million merged systems. Our calculation only accounts for BBHs from field binaries, and we only track systems where both stars form a BH, where the binary does not undergo a stellar merger, and where the binary survives the natal kicks. As such, we do not account for BHs with lower mass companions (WDs, NSs, or low-mass stars). Thousands of BHs with stellar companions will likely by detected by the astrometric *Gaia* satellite (Mashian & Loeb 2017; Breivik et al. 2017) and possibly their Hα emission (Casares 2018). Given that even at the lowest metallicity, only 8 per cent of the massive binaries turn into a BH binary, there could be 10 times more BHs that have been kicked out of a binary. As such, the first electromagnetic detection of isolated BHs in the MW will most likely be a single BH. A more accurate determination of their masses, proper motions, spatial distribution, and, ultimately, detectability is left for a further study.

6 CONCLUSIONS

In this paper, we provide the first estimates of the isolated BH population resulting from BBH systems. It is based on the combination of a high-resolution cosmological simulation of a MW-mass galaxy and a binary population synthesis model. The simulation provides a physically motivated, metallicity-dependent star formation history as well as a complete description of the galactic morphology and merger activity over time. The simulation models both resolved and unresolved turbulent metal diffusion, which provides a realistic metal *distribution*, rather than just the average value (Ma et al. 2017; Escala et al. 2018). The stellar metallicity is a key parameter for massive binary evolution. Using a standard binary evolution model, we compute a metallicity-dependent library of BBHs for 13 metallicities between $Z = 0.0005\,Z_\odot$ and $Z = 1.6\,Z_\odot$, then match them to the stars in the simulation. This provides a self-consistent distribution of BHs within 300 kpc of the centre of the galaxy, including their localization, masses, orbital properties, and the properties of their stellar progenitors. The main properties of these binaries are summarized below:

(i) We find that 6.8×10^5 BBH binaries have already merged in our MW model and 1.2×10^6 systems are still in BBHs. Our MW-like galaxy has turned 0.07 per cent of its $z = 0$ stellar mass into BBHs, including the ones that have merged already.

(ii) The mean progenitor metallicity of the merged (unmerged) systems is $Z = 0.13$ (0.25) $Z_\odot$, and only 1 per cent of the binaries come from supersolar metallicity progenitors. This means that most of the stellar mass in MW-mass galaxies is effectively unavailable for the formation of BH binaries. The binary systems thus strongly trace star formation around $z \simeq 2$, while the already-merged systems mostly trace star formation from $z > 2$.

(iii) The strong dependence on low-metallicity star formation results in half of the binaries (merged or not) being located beyond 10 kpc of the galactic centre. In comparison, 90 per cent of the stellar mass is located within 10 kpc. The galactic halo, streams, and satellite galaxies are rich in BBHs.

(iv) We find about 40 000 merged binaries with masses comparable to the mergers detected with the first LIGO detection. Consistent with Lamberts et al. (2016), we find that these systems were typically formed outside of the MW and are now in the halo or still in their host satellite galaxy. They stem from progenitors with metallicity below $0.1\,Z_\odot$.

(v) The detection of merged and unmerged BBHs without stellar companions will remain a challenge for the foreseeable future. Our binary evolution model predicts that 25 binaries could be detected with *LISA*, but that most of the binaries have an orbit that is too wide and/or are too distant for *LISA* to detect their gravitational wave emission. Depending on the radiation efficiency and accretion

mechanism, the accretion of surrounding gas could lead to detections with all-sky radio or X-ray surveys like *SKA* or *eROSITA*. A few systems may be detected by microlensing surveys. In any case, observational constraints will lead to a better understanding of massive binary evolution, which is still poorly understood.

(vi) About a third of the BBHs were not initially formed in the galaxy, and have been brought in by the accretion of satellite dwarf galaxies. 60 per cent of the systems with total mass above 60 $M_\odot$ were formed ex situ. This highlights the importance of accounting for galactic mergers when predicting BH populations and merger rates in MW-mass galaxies.

(vii) The mean total mass is 29 $M_\odot$ for the merged systems and a total mean mass of 23 $M_\odot$ for the binary systems. Roughly 10 per cent of the systems have total masses above 50 $M_\odot$ and about one per cent of the systems have a mass above 80 $M_\odot$.

(viii) We provide online data including a table of the star formation rate as a function of metallicity and time. The latter can be used to combine the galaxy model with different binary evolution models. We also provide the properties of the BBHs from our model, which can be used to derive observational signatures from lensing and/or accretion.

This paper provides the first estimate of the population of BBHs and their merger remnants in a MW-mass galaxy that incorporates a realistic star-formation history and galactic halo structure and merger history based on a hydrodynamic simulation. This allows us to reliably estimate low-metallicity star formation and localize BBHs. Based on this precise galactic model, future detections of such systems in our vicinity will then allow us to constrain key parameters of massive stellar binary evolution.

ACKNOWLEDGEMENTS

Astrid Lamberts would like to thank V. Ravi, H. Vedantham, M. Heida, C. Henderson, Y. Shvarzvald, S. Novati, and S. Taylor for discussions about observational implications of this work and D. Clausen for his help with the BPS models. Numerical calculations were run on the Caltech compute cluster 'Wheeler,' allocations from XSEDE TG-AST130039and PRAC NSF.1713353 supported by the NSF, and NASA HEC SMD-16-7592.

Support for AL and PFH was provided by an Alfred P. Sloan Research Fellowship, NASA ATP Grant NNX14AH35G, and NSF Collaborative Research Grant 1715847 and CAREER grant 1455342. Support for SGK was provided by NASA through Einstein Postdoctoral Fellowship grant number PF5-160136 awarded by the Chandra X-ray Center, which is operated by the Smithsonian Astrophysical Observatory for NASA under contract NAS8-03060. EQ was supported in part by NSF grant AST-1715070 and a Simons Investigator Award from the Simons Foundation. JSB was supported by NSF grant AST-1518291 and by NASA through *HST* theory grants (programmes AR-13921, AR-13888, and AR-14282.001) awarded by STScI, which is operated by the Association of Universities for Research in Astronomy (AURA), Inc., under NASA contract NAS5-26555. CAFG was supported by NSF through grants AST-1412836, AST-1517491, AST-1715216, and CAREER award AST-1652522 and by NASA trough grant NXX-15AB22G. AW was supported by NASA through grants *HST*-GO-14734 and *HST*-AR-15057 from STScI. DK acknowledges support from NSF grants AST-1412153 and AST-1715101 and the Cottrell Scholar Award from the Research Corporation for Science Advancement. RES was supported by an NSF Astronomy & Astrophysics Postdoctoral Fellowship under grant AST-1400989. This study was initiated during K. Drango's 'Freshman Summer Research Internship', organized by the Caltech Center for Diversity. We thank Kacper Kowalik and the whole yt hub team where our dataset is hosted. It is supported in part by the Gordon and Betty Moore Foundation's Data Drive Discovery Initiative through grant GBMF4561 to Matthew Turk and the National Science Foundation under Grant number ACI-1535651.

REFERENCES

Abbott B. P. et al., 2016a, Phys. Rev. X, 6, 041015
Abbott B. P. et al., 2016b, Phys. Rev. Lett., 116, 061102
Abbott B. P. et al., 2016c, ApJS, 227, 14
Abbott B. P. et al., 2016d, ApJ, 818, L22
Abbott B. P. et al., 2017a, Phys. Rev. Lett., 118, 221101
Abbott B. P. et al., 2017b, Phys. Rev. Lett., 119, 141101
Abbott B. P. et al., 2017c, ApJ, 851, L35
Agol E., Kamionkowski M., 2002, MNRAS, 334, 553
Agol E., Kamionkowski M., Koopmans L. V. E., Blandford R. D., 2002, ApJ, 576, L131
Amaro-Seoane P. et al., 2017, preprint (arXiv:1702.00786)
Anglés-Alcázar D., Faucher-Giguère C.-A., Kereš D., Hopkins P. F., Quataert E., Murray N., 2017, MNRAS, 470, 4698
Badenes C. et al., 2018, ApJ, 854, 147
Baldry I. K., Glazebrook K., Driver S. P., 2008, MNRAS, 388, 945
Behroozi P. S., Wechsler R. H., Conroy C., 2013, ApJ, 770, 57
Belczynski K., Kalogera V., Bulik T., 2002, ApJ, 572, 407
Belczynski K., Taam R. E., Kalogera V., Rasio F. A., Bulik T., 2007, ApJ, 662, 504
Belczynski K., Kalogera V., Rasio F. A., Taam R. E., Zezas A., Bulik T., Maccarone T. J., Ivanova N., 2008, ApJS, 174, 223
Belczynski K., Bulik T., Fryer C. L., Ruiter A., Valsecchi F., Vink J. S., Hurley J. R., 2010a, ApJ, 714, 1217
Belczynski K., Benacquista M., Bulik T., 2010b, ApJ, 725, 816
Belczynski K., Holz D. E., Bulik T., O'Shaughnessy R., 2016, Nature, 534, 512
Bonaca A., Conroy C., Wetzel A., Hopkins P. F., Kereš D., 2017, ApJ, 845, 101
Breivik K., Chatterjee S., Larson S. L., 2017, ApJ, 850, L13
Casares J., 2018, MNRAS, 473, 5195
Casares J., Jonker P. G., Israelian G., 2017, Handbook of Supernovae. Springer International Publishing AG, Cham, Switzerland, p. 1499
Chakrabarti S., Chang P., O'Shaughnessy R., Brooks A., Shen S., Bellovary J., Gladysz W., Belczynski C., 2017, ApJ, 850, L4
Christian P., Loeb A., 2017, MNRAS, 469, 930
Corbel S. et al., 2015, Proceedings of Advancing Astrophysics with the Square Kilometre Array (AASKA14). Giardini Naxos, Italy, p. 53
Corral-Santana J. M., Casares J., Muñoz-Darias T., Bauer F. E., Martínez-Pais I. G., Russell D. M., 2016, A&A, 587, A61
de Mink S. E., Belczynski K., 2015, ApJ, 814, 58
de Mink S. E., Sana H., Langer N., Izzard R. G., Schneider F. R. N., 2014, ApJ, 782, 7
Dominik M., Belczynski K., Fryer C., Holz D. E., Berti E., Bulik T., Mandel I., O'Shaughnessy R., 2012, ApJ, 759, 52
Dominik M., Belczynski K., Fryer C., Holz D. E., Berti E., Bulik T., Mandel I., O'Shaughnessy R., 2013, ApJ, 779, 72
Elbert O. D., Bullock J. S., Kaplinghat M., 2018, MNRAS, 473, 1186
Eldridge J. J., Stanway E. R., 2016, MNRAS, 462, 3302
Eldridge J. J., Tout C. A., 2004, MNRAS, 353, 87
Escala I. et al., 2018, MNRAS, 474, 2194
Fender R. P., Maccarone T. J., Heywood I., 2013, MNRAS, 430, 1538
Fryer C. L., 1999, ApJ, 522, 413
Fryer C. L., Belczynski K., Wiktorowicz G., Dominik M., Kalogera V., Holz D. E., 2012, ApJ, 749, 91
Garcia Pérez A. E. et al., 2018, ApJ, 852, 91
Garrison-Kimmel S. et al., 2017, preprint (arXiv:1712.03966)
Geen S., Rosdahl J., Blaizot J., Devriendt J., Slyz A., 2015, MNRAS, 448, 3248

Harris J., Zaritsky D., 2009, AJ, 138, 1243
Heger A., Fryer C. L., Woosley S. E., Langer N., Hartmann D. H., 2003, ApJ, 591, 288
Hopkins P. F., 2015, MNRAS, 450, 53
Hopkins P. F., Kereš D., Oñorbe J., Faucher-Giguère C.-A., Quataert E., Murray N., Bullock J. S., 2014, MNRAS, 445, 581
Hopkins P. F. et al., 2018, MNRAS, 480, 800
Hurley J. R., Tout C. A., Pols O. R., 2002, MNRAS, 329, 897
Ioka K., Matsumoto T., Teraki Y., Kashiyama K., Murase K., 2017, MNRAS, 470, 3332
Ivanova N., Taam R. E., 2004, ApJ, 601, 1058
Iwamoto K., Brachwitz F., Nomoto K., Kishimoto N., Umeda H., Hix W. R., Thielemann F.-K., 1999, ApJS, 125, 439
Izzard R. G., Tout C. A., Karakas A. I., Pols O. R., 2004, MNRAS, 350, 407
Janka H.-T., 2013, MNRAS, 434, 1355
Kinugawa T., Inayoshi K., Hotokezaka K., Nakauchi D., Nakamura T., 2014, MNRAS, 442, 2963
Klein A. et al., 2016, Phys. Rev. D, 93, 024003
Kroupa P., 2001, MNRAS, 322, 231
Lamberts A., Garrison-Kimmel S., Clausen D. R., Hopkins P. F., 2016, MNRAS, 463, L31
Liu J., Zhang Y., 2014, PASP, 126, 211
Ma X., Hopkins P. F., Faucher-Giguère C.-A., Zolman N., Muratov A. L., Kereš D., Quataert E., 2016, MNRAS, 456, 2140
Ma X., Hopkins P. F., Wetzel A. R., Kirby E. N., Anglés-Alcázar D., Faucher-Giguère C.-A., Kereš D., Quataert E., 2017, MNRAS, 467, 2430
Maccarone T. J., 2005, MNRAS, 360, L30
Mackereth J. T. et al., 2017, MNRAS, 471, 3057
Madau P., Dickinson M., 2014, ARA&A, 52, 415
Maggiore M., 2008, Gravitational Waves. Oxford Univ. Press, Oxford
Mandel I., 2016, MNRAS, 456, 578
Mandel I., de Mink S. E., 2016, MNRAS, 458, 2634
Mapelli M., 2016, MNRAS, 459, 3432
Mapelli M., Giacobbo N., Ripamonti E., Spera M., 2017, MNRAS, 472, 2422
Marchant P., Langer N., Podsiadlowski P., Tauris T. M., Moriya T. J., 2016, A&A, 588, A50
Marigo P., 2001, A&A, 370, 194
Mashian N., Loeb A., 2017, MNRAS, 470, 2611
Mennekens N., Vanbeveren D., 2014, A&A, 564, A134
Mirhosseini A., Moniez M., 2017, preprint (arXiv:1711.10898)
Muratov A. L., Kereš D., Faucher-Giguère C.-A., Hopkins P. F., Quataert E., Murray N., 2015, MNRAS, 454, 2691
Nelemans G., Yungelson L. R., Portegies Zwart S. F., 2001, A&A, 375, 890
Nomoto K., Tominaga N., Umeda H., Kobayashi C., Maeda K., 2006, Nucl. Phys. A, 777, 424
O'Leary R. M., Meiron Y., Kocsis B., 2016, ApJ, 824, L12
Perna R., Narayan R., Rybicki G., Stella L., Treves A., 2003, ApJ, 594, 936
Peters P. C., Mathews J., 1963, Phys. Rev., 131, 435
Planck Collaboration XIII, 2016, A&A, 594, A13
Porcel C., Garzon F., Jimenez-Vicente J., Battaner E., 1998, A&A, 330, 136
Postnov K. A., Yungelson L. R., 2014, Living Rev. Relativ., 17, 3
Repetto S., Davies M. B., Sigurdsson S., 2012, MNRAS, 425, 2799
Rodriguez C. L., Morscher M., Pattabiraman B., Chatterjee S., Haster C.-J., Rasio F. A., 2015, Phys. Rev. Lett., 115, 051101
Ruiter A. J., Belczynski K., Benacquista M., Larson S. L., Williams G., 2010, ApJ, 717, 1006
Samland M., 1998, ApJ, 496, 155
Sana H. et al., 2012, Science, 337, 444
Sanderson R. E. et al., 2017, preprint (arXiv:1712.05808)
Sanderson R. E. et al., 2018, preprint (arXiv:1806.10564)
Schneider R., Graziani L., Marassi S., Spera M., Mapelli M., Alparone M., de Bennassuti M., 2017, MNRAS, 471, L105
Sesana A., 2016, Phys. Rev. Lett., 116, 231102
Seto N., 2016, MNRAS, 460, L1
Shapiro S. L., Teukolsky S. A., 1983, Black Holes, White Dwarfs, and Neutron Stars: The Physics of Compact Objects. Wiley VCH, Germany
Stevenson S., Ohme F., Fairhurst S., 2015, ApJ, 810, 58
Sukhbold T., Ertl T., Woosley S. E., Brown J. M., Janka H.-T., 2016, ApJ, 821, 38
Su K.-Y., Hopkins P. F., Hayward C. C., Faucher-Giguère C.-A., Kereš D., Ma X., Robles V. H., 2017, MNRAS, 471, 144
van den Heuvel E. P. J., 1992, Technical Report, Endpoints of Stellar Evolution: The Incidence of Stellar Mass Black Holes in the Galaxy. ESA, The Netherlands
van den Hoek L. B., Groenewegen M. A. T., 1997, A&AS, 123, 305
Voss R., Tauris T. M., 2003, MNRAS, 342, 1169
Webbink R. F., 1984, ApJ, 277, 355
Wetzel A. R., Hopkins P. F., Kim J.-h., Faucher-Giguère C.-A., Kereš D., Quataert E., 2016, ApJ, 827, L23
Wyrzykowski L. et al., 2011, MNRAS, 416, 2949
Wyrzykowski Ł. et al., 2016, MNRAS, 458, 3012-6

This paper has been typeset from a TEX/LATEX file prepared by the author.